Central European Journal of Energetic Materials
ISSN 1733-7178; e-ISSN 2353-1843

Cent. Eur. J. Energ. Mater. 2019, *16*(2): 259-280; DOI: 10.22211/cejem/110025
Article is available in PDF-format, in colour, at:
http://www.wydawnictwa.ipo.waw.pl/cejem/Vol-16-Number-2-2019/CEJEM_00959.pdf

Research paper

Studies on the Effect of a Covalently Bonded PGN Based Reactive Plasticizer on the Thermal Decomposition Behaviour of Glycidyl Azide Polymer

Asghar Bodaghi, Mansour Shahidzadeh*
Department of Chemistry and Chemical Engineering Faculty of Material and Chemical Engineering, Malek-Ashtar University of Technology, PO Box: 16765-3454, Lavizan, Tehran, Iran
**E-mail:* mshahidzadeh@yahoo.com

Abstract: Plasticizers are one of the additives that are added to polymers to increase the plasticity or decrease the viscosity of the material. Here, we have synthesized and characterized a new PGN-based reactive energetic plasticizer that has an oligomeric structure. The reactive energetic plasticizer can be grafted onto glycidyl azide polymer *via* a Cu-free Huisgen azide-alkyne 1,3-dipolar cycloaddition. The effect of the covalently bonded PGN-based plasticizer on the thermal properties of GAP-g-PGN copolymer has been investigated through thermogravimetric analysis and differential scanning calorimetry. The results indicate that the glass transition temperature of the prepolymer is decreased from –47.8 to –50.7 °C. Also, the kinetics of the thermal behaviour of GAP-g-PGN copolymer was determined by the application of the Kissinger and FWO kinetic models. The activation energies calculated by the Kissinger method were 165 and 188 kJ/mol for peak 1 and peak 2, respectively. Furthermore, the critical temperature (T_b) of thermal explosion for this energetic copolymer was estimated to be 182 °C.

Keywords: plasticizer, reactive plasticizer, glycidyl azide polymer, kinetic study, activation energy

Acronyms:

EPs	Energetic plasticizers
GAP	Glycidyl azide polymer
GAP-g-PGN	Copolymer of poly(glycidyl azide) and poly(glycidyl nitrate)
M_n	Number average molar mass (molecular weight) [g/mol]
M_w	Mass average molar mass [g/mol]
PDI	M_w/M_n ratio
PGA	Poly(glycidyl azide)
PGN	Poly(glycidyl nitrate)
PTMPGN	Propargyl-terminated poly(glycidyl nitrate) ester
REP	Reactive energetic plasticizer
T_g	Glass transition temperature [°C]

1 Introduction

A plasticizer is a low to medium molecular weight substance that is introduced into a polymer for control of its properties. Plasticizers are introduced into polymers to increase their flexibility and improve processability [1]. The addition of a plasticizer causes a reduction in the cohesive intermolecular forces along the polymer chains. The chains can then move more freely relative to one another, and the stiffness of the polymer is reduced [2].

Plasticizers are one of the additives that are used in propellant formulations. On their addition to the propellant, they impart lower viscosity for mixing and greater pot life [3]. Plasticizers when added to polymers significantly reduce the brittleness by penetrating deep inside the polymer matrix and reducing the cohesive forces between polymers and increasing the free volume. This causes an increase in segment mobility, leading to a reduction of T_g. The extent to which a plasticizer reduces the T_g of a polymer is used as a measure of plasticizer efficiency [4].

The molecular weight of plasticizers may vary from 200 to 2000, and thus vary their properties. Low molecular weight plasticizers tend to be volatile whereas higher molecular weight plasticizers are more viscous. Consequently plasticizers having a molecular weight in the range of 400-1000 (plasticizers which have an oligomeric structure) are preferred.

Energetic plasticizers (EPs) are defined as liquid materials having a positive heat of explosion [5]. These compounds have been used as one of the ingredients in solid propellants and plastic bonded explosives (PBX) formulations. Energetic plasticizers can improve the mechanical and thermal properties

of propellants, and can also enhance their energetic performance [6-9].

Migration is a common problem observed with plasticizers. Plasticizers incorporated into polymers migrate and exude slowly from the polymer matrix, which is undesirable even under moderate storage conditions [7, 9-12]. Loss of plasticizer is undesirable, leading to a brittle and unusable high energy material, as well as contamination of the surrounding environment [9] and increased hazardous properties of the energetic matrix.

A variety of approaches has been used [11, 13, 14] to reduce the migration, for example, increasing the molecular weight of the plasticizers, adding nano-sized inorganic particles to polar plasticizer molecules and increasing the compatibility of the plasticizer and polymer matrix. In all of these approaches, the main interaction between the polymer and the plasticizer is a kind of physical bonding, and the problem of plasticizer migration from the polymer still remains a major problem.

Recently, the use of reactive plasticizers and chemically bonding plasticizers to the polymer main chains has attracted the attention of researchers. One of the types of reactive plasticizers is an alkynyl compound, which can react with an azido-containing energetic prepolymer through an azide-alkyne click reaction. Thereby, the reactive plasticizer solves the conventional problem of plasticizers and reduces the migration of plasticizers. The reactive energetic plasticizer (REP) comprises a high energy functional group as well as a functional group which can react with a side chain of a prepolymer [15].

Within the last two decades, attention has been focused on developing several azido energetic polymers including azide polymers; glycidyl azide polymers (GAPs); poly(3-azidomethyl3-methyl oxetane) [poly(AMMO)]; poly[3,3-bis(azidomethyl) methyl oxetane] [poly-(BAMO)]. Of these azido polymers, glycidyl azide polymer (GAP) or poly(glycidyl azide) (PGA) is one of the most important and prominent azide polymers that is characterized by pendent azidomethyl groups on the main polyether chain. GAP is a high energy potential material with a high positive heat of formation (957 kJ/kg) and low detonation sensitivity, and is considered both a monopropellant and a polymeric binder. GAP has a low glass-transition temperature, low viscosity, high density compared to the same characteristics of other rocket propellant binders and good compatibility with all high-energy oxidizers. Because of its unique properties GAP is used extensively as a highly energetic binder-*cum*-plasticizer to increase burning and specific impulse of propellants [16].

In the present study, we have synthesized a typical REP that can be bonded onto the glycidyl azide polymer, through catalyst-free click chemistry, to form (GAP-g-PGN) copolymer, as a promising binder for cast cure propellants

and plastic bonded explosives.

Thermal decomposition behaviour of the non-migrating plasticized glycidyl azide polymer was investigated using simultaneous thermogravimetry-differential scanning calorimetry (TG/DSC). Also, in this study, the thermokinetic parameters of the non-isothermal decomposition of the (GAP-g-PGN) copolymer have been determined.

2 Experimental

2.1 Materials

GAP (M_n = 1435, M_w/M_n = 1.64) was synthesized in a two-step reaction according to the method in the literature [17, 18]. Glycidyl nitrate (GN) was synthesized according to the method reported elsewhere [19]. Epichlorohydrin (99%, Merck), propargylic alcohol (99%, Merck), succinic anhydride (97%, Fluka), $BF_3{\cdot}OEt_2$ (50%, Merck), thionyl chloride (99%, Merck), fuming nitric acid (63%, Merck), potassium nitrate (99%, Merck), methanol (99.5%, Merck), methylene chloride and dimethylformamide (DMF) were obtained from Sigma-Aldrich.

2.2 Instruments and measurements

The IR spectra were recorded with a Nicolet 800 spectrometer in the range 400-4000 cm^{-1}. ^1H NMR spectra were recorded with a Bruker DPX-250 instrument operating at 250.13 MHz and using $CDCl_3$ as solvent; chemical shifts were reported in δ (ppm) from TMS. Thermogravimetric (TG), isothermal TG and differential scanning calorimetric (DSC) analyses were carried out using a Perkin Elmer, STA 6000 instrument with alumina pans under an argon atmosphere at temperature programmed rates of 5, 10, 15 and 20 °C/min, from room temperature to 450 °C. The samples masses were about 12 mg. The glass transition temperature (T_g) measurements were performed using a DSC 200F3 under a nitrogen flow of 20.0 mL/min with a heating rate of 10 °C/min, from –100 to 50 °C. The T_g value was computed as the midpoint of the heat capacity increase. Gel permeation chromatography (GPC) was conducted using 10 µm PL gel columns using a GPC Agilent 1100 (USA) instrument with a refractive index detector using an Agilent PLgel 5 µm mixed-C, 300 mm × 7.5 mm column; THF was used as the solvent and injected at 30 °C at a rate of 1 mm/min and calibrated with polystyrene as standard.

2.3 Methods

2.3.1 Synthesis of propargyl-terminated poly(glycidyl nitrate) ester (PTMPGN)

For the synthesis of propargyl-terminated MPGN ester (PTMPGN), PCPCl (1.05 g, 6 mmol) in CH_2Cl_2 (50 mL) was added dropwise to a stirred solution of MPGN (3 g, 4 mmol hydroxyl groups) and DMF (0.65 mL, 13 mmol) in dry CH_2Cl_2 (45 mL) under a nitrogen atmosphere in an ice bath; the duration of this process was more than 0.5 h. The reaction mixture was stirred at room temperature for 11 h and then repeatedly washed with water. The organic layer was dried with $MgSO_4$, filtered and evaporated *in vacuo* to produce 3 g of pale yellow PTMPGN, in 75% yield. The analytical results were as follows:

- **^{1}H NMR** (250 MHz, $CDCl_3$, ppm) δ: 4.95(s, 2H, ≡C–CH_2–O), 4.51-4.73(m, 2H, –CHC***H*****$_2$**ONO_2), 3.37(s, 1H, HC≡), 3.4-3.79(m, 6H, chain –CH_2O–, –CH– group, and –OCH_3), 2.5-2.68(m, 4H, $COCH_2CH_2CO$),
- **FTIR** (KBr, cm^{-1}) *v:* 3444, 3296, 2129, 1740, 1636, 1281, 1147 and 859,
- **GPC analysis** revealed a molecular weight (M_n) of 731 g/mol and molecular weight distribution (M_w/M_n) of 1.4 (see Figure 1).

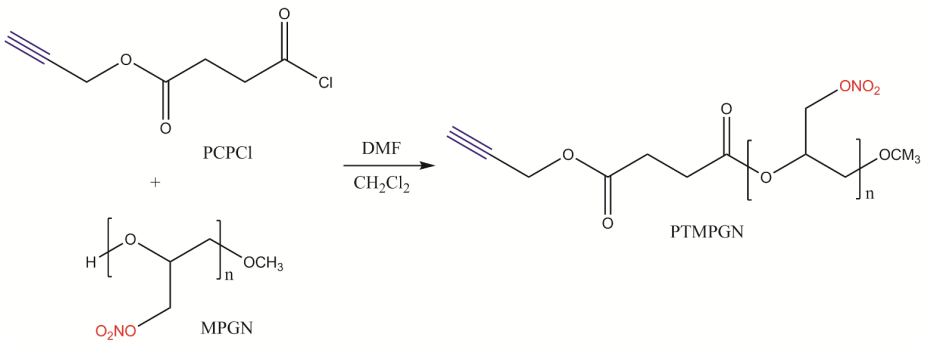

Figure 1. Synthetic route for the propargyl-terminated, methylated poly(glycidyl nitrate)

2.3.2 Synthesis of GAP-g-PGN

GAP (1.5 g, 1 mmol) was placed in a round-bottom flask with stirrer and PTMPGN plasticizer (2.2 g, 3 mmol) was added. The reaction mixture was heated to 60 °C with stirring in an oil bath for 48 h. In this reaction, about 20% of the azide groups of GAP reacted. The analytical results were as follows:

- **^{1}H NMR** (250 MHz, $CDCl_3$, ppm) δ: 4.51-4.73(m, 2H, –CH_2ONO_2); 3.29-3.79(m, 3H, chain –CH_2O–, –CH– group, –$OCCH_2CO$– and –OCH_3);

3.4(2H, $-CH_2N_3$); 3.66(3H, CH_2–CH–O); 7.29 and 7.91(s, 1H, HC=C (triazole ring)),

– **FTIR** (KBr, cm^{-1}) *v:* 3428, 2103, 1736, 1634, 1281, 1119 (see Figure 2).

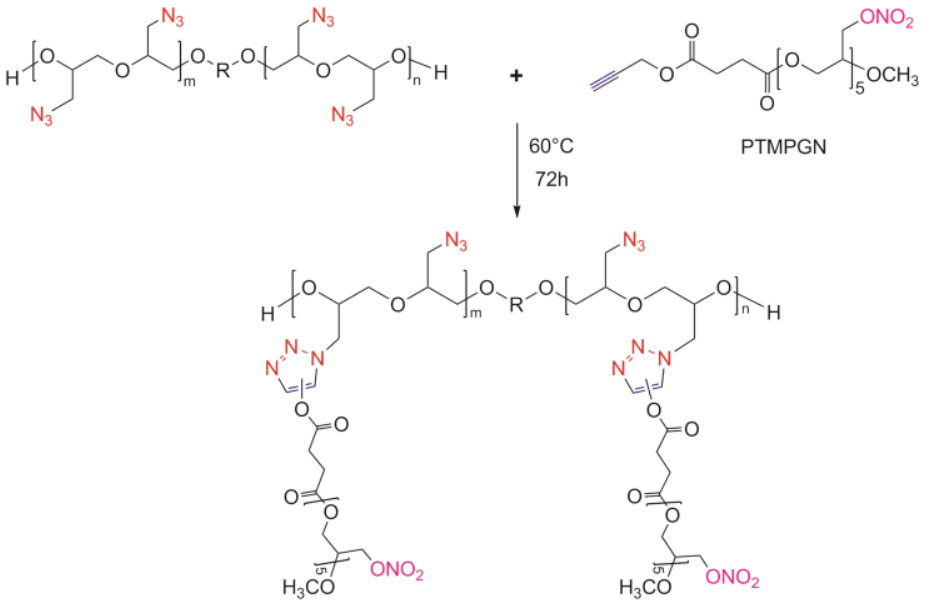

Figure 2. Synthetic process for GAP-g-PGN, where R = $(CH_2)_4$

3 Results and Discussion

3.1 Characterization

The synthesized PTMPGN, GAP and GAP-g-PGN copolymer were charachterized by FT-IR spectroscopy, GPC, DSC. Figure 3 shows the IR spectra of the plasticizer PTMPGN, GAP and modified GAP (GAP-g-PGN). The analytical results were as follows:

– **IR** (cm^{-1}): 3296(≡C–H), 2129(C≡C), 1740(–C=O), 1636, 1281(NO_2), 1147(C–O–C), 855(O–N).

In the FT-IR spectrum of GAP-g-PGN, the peak absorption of (≡C–H) had disappeared whereas the absorption peaks of other functional groups appeared. Thus, the click reaction between azide groups in GAP and the alkynyl group in the plasticizer was confirmed in GAP-g-PGN (see Figure 3).

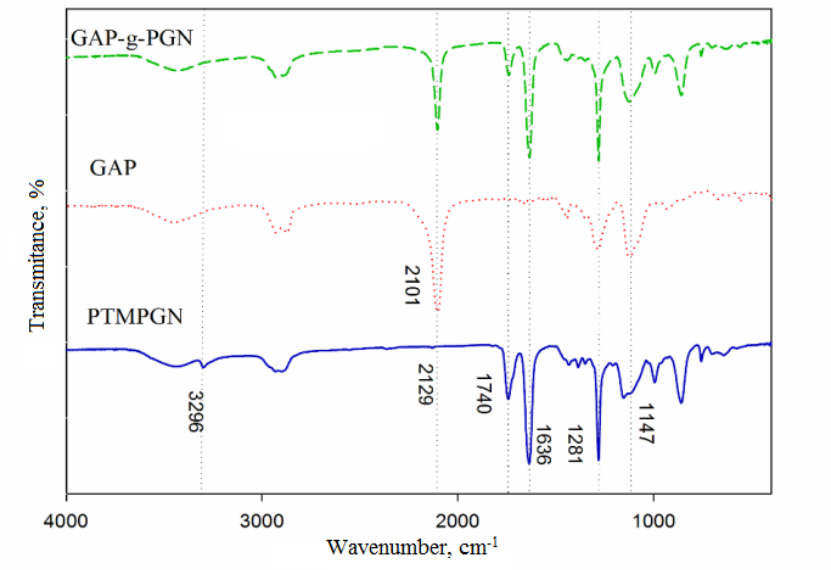

Figure 3. Comparison of FTIR spectra of PTMPGN, GAP, and GAP-g-PGN

In the ^{1}H NMR spectrum of GAP-g-PGN, two peaks appeared as singlets at 7.29 and 7.91 ppm, which were assigned to the triazole ring of the two isomeric compounds, respectively. Thus, the 1,3 dipolar cycloaddition reaction between azide groups of GAP and the alkynyl group of the reactive plasticizer was confirmed (see Figure 4).

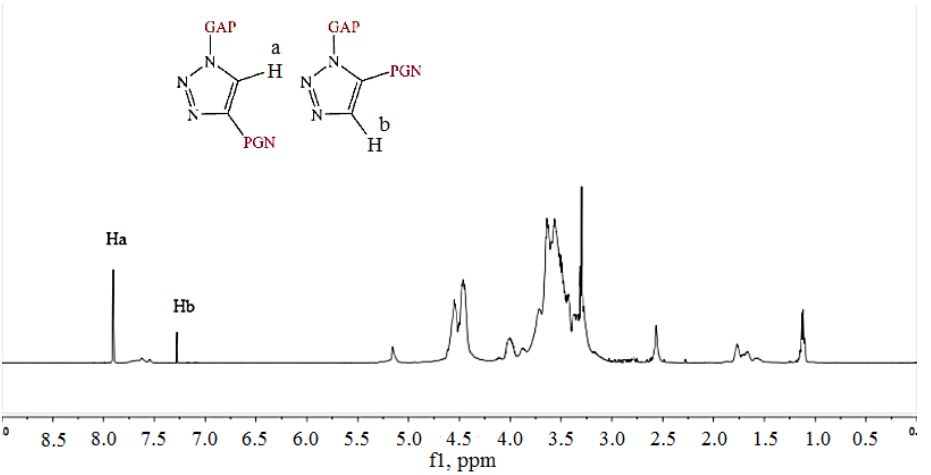

Figure 4. ^{1}H NMR spectra of GAP-g-PGN copolymer

The M_n, M_w, and PDI (M_w/M_n) values of the synthesized PTMPGN, GAP and GAP-g-PGN are listed in Table 1. The M_n values of GAP-g-PGN was around 950 g/mol, with a PDI value of 1.9.

Table 1. Composition of PTMPGN, GAP, and GAP-g-PGN

Molecular weight	PTMPGN	GAP	GAP-g-PGN
M_n [g/mol]	731	1435	951
M_w [g/mol]	1028	2362	1813
M_n/M_w	1.406	1.64	1.9

Considerable data have been produced for the effect of plasticizer on the T_g values of polymer systems and have appeared in the literature [20-24]. PTMPGN is a reactive energetic plasticizer. Figure 5 shows the DSC thermograms of PTMPGN, GAP, and GAP-g-PGN. The glass-transition temperatures (T_g values) of the synthesized compounds are listed in Table 2. As shown in Table 2, the glass transition temperatures of PTMPGN, GAP, and GAP-g-PGN were –66.5, –47.8 and –50.7 °C, respectively. The plasticizer was used to reduce the T_g of GAP and to increase the processability of the binder. As may be seen, the T_g value of the modified GAP, relative to GAP, is reduced (see Figure 5).

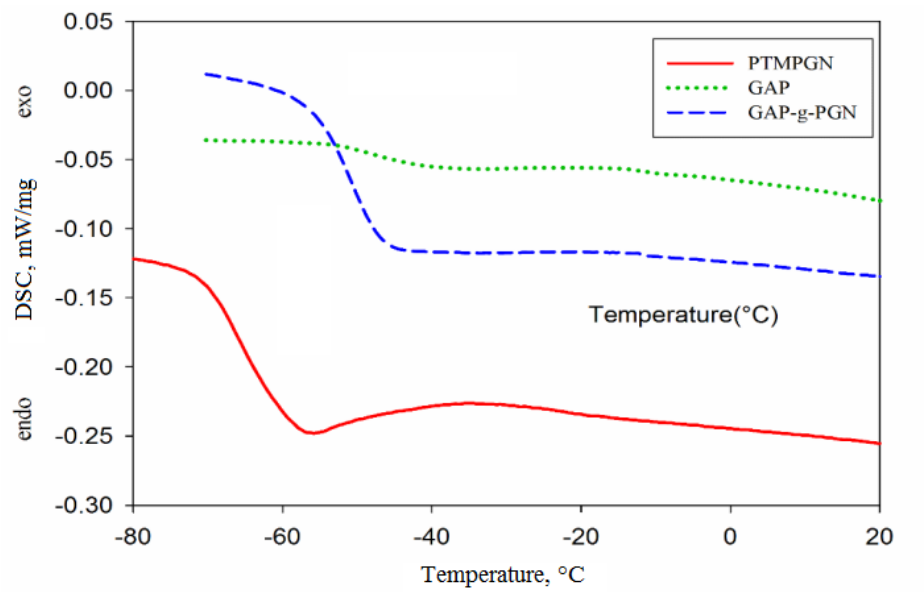

Figure 5. DSC thermograms of PTMPGN, GAP, and GAP-g-PGN at 10 °C/min

Table 2. T_g values of PTMPGN, GAP, and GAP-g-PGN

Compound	PTMPGN	GAP	GAP-g-PGN
T_g [°C]	–66.5	–47.8	–50.7

3.2 Thermal decomposition of GAP-g-PGN

Thermal analysis is frequently used in propellant research. Thermal decomposition can be correlated with important performance parameters, such as heat of explosion, detonation velocity, and detonation energy [25]. So, it was necessary to understand the thermal decomposition process of GAP-g-PGN. Figure 6 shows the thermal curves of PTMPGN, GAP, and GAP-g-PGN recorded at 20 °C/min.

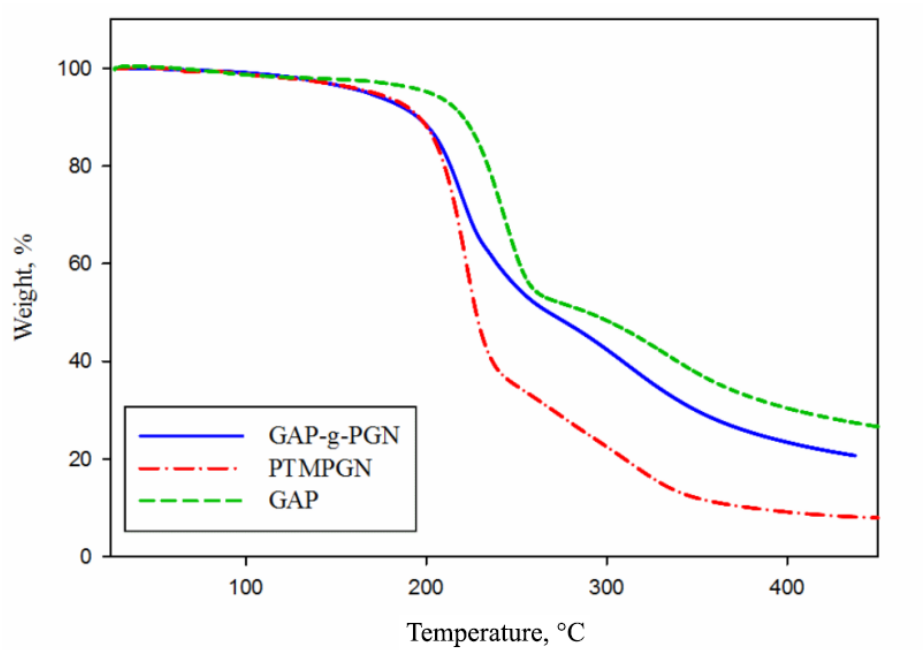

Figure 6. TGA curves of PTMPGN, GAP, and GAP-g-PGN

In the TGA curve of PTMPGN, two characteristic mass loss steps were observed. The first step (a) started at 170 °C and ended at 250 °C, and corresponded to the decomposition of $–ONO_2$ [26]. The second stage involved the decomposition of the polyether skeleton between 250 and 430 °C. These two weight loss stages are depicted in the DTG curve (Figure 7).

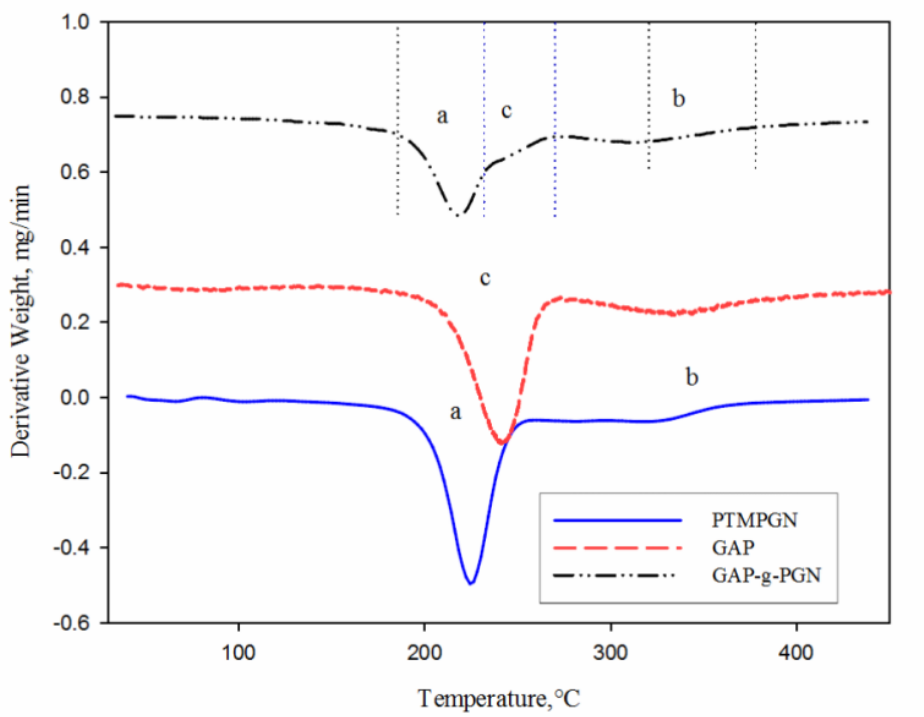

Figure 7. DTG curves of PTMPGN, GAP, and GAP-g-PGN

The TGA curve of GAP-g-PGN exhibited three mass loss steps, which are shown in the DTG curve of GAP-g-PGN (Figure 7). The first stage (a) started at 170 °C and ended at 230 °C. This corresponds to the decomposition of $–ONO_2$. Thermal analysis of GAP showed that there is no decomposition peak up to 190 °C, and the onset of decomposition of GAP only starts above 190 °C [27]. So, the second stage (c) corresponds to the decomposition of $–N_3$. The third stage corresponds to the decomposition of the polyether skeleton (b) (Figure 7).

We should note that two types of energetic group, $–ONO_2$ and $–N_3$, were present in the modified GAP. The decompositions of the nitrate and azide groups in GAP-g-PGN approximately overlapped. By investigating the DTG of GAP-g-PGN, we found that the degradation stage of GAP-g-PGN between 170 and 250 °C corresponded to the decomposition of both $–ONO_2$ and $–N_3$ and the stage between 250 and 350 °C corresponded to the decomposition of the polyether skeleton of GAP-g-PGN (see Figure 7).

To study the various steps in the decomposition of GAP-g-PGN, the DTG curves of GAP-g-PGN at different heating rates were plotted as shown in Figure 8. Three stages (a, c and b, respectively), due to the decomposition of $–ONO_2$, $–N_3$ groups and the polyether skeleton in the plasticizer and GAP became apparent (see Figure 8). The DSC thermogram of GAP-g-PGN showed an exothermic decomposition, with a peak temperature at 204 °C, accompanied by a heat release of 1795 J/g (see Figure 9). The effect of heating rate on the peak temperature and the onset temperature of the first exothermic decomposition on the DSC thermograms of GAP-g-PGN shows that with increasing heating rate, the decomposition peak shifted towards higher temperatures (see Figure 10).

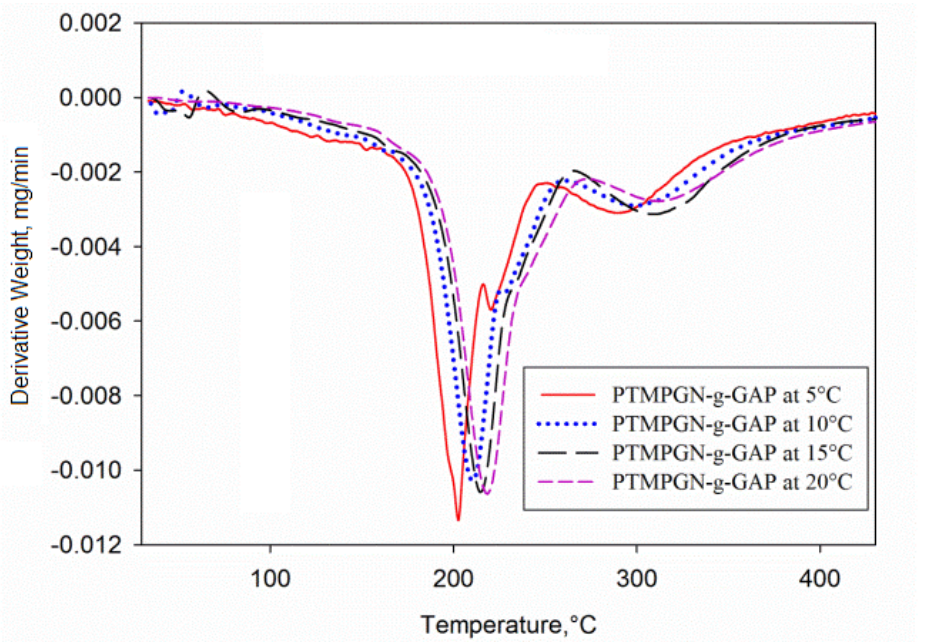

Figure 8. DTG curves of GAP-g-PGN samples at various heating rates: 5, 10, 15, and 20 °C/min

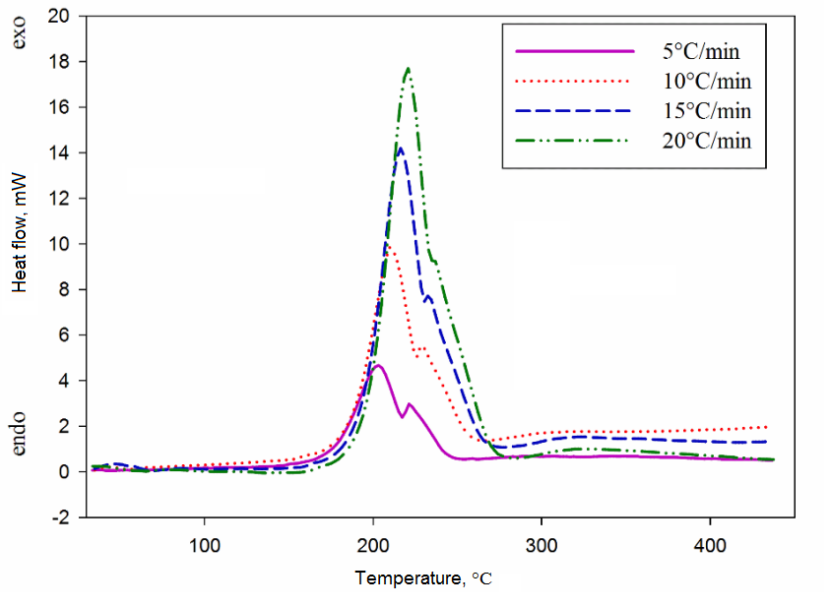

Figure 9. DSC thermograms of GAP-g-PGN at different heating rates

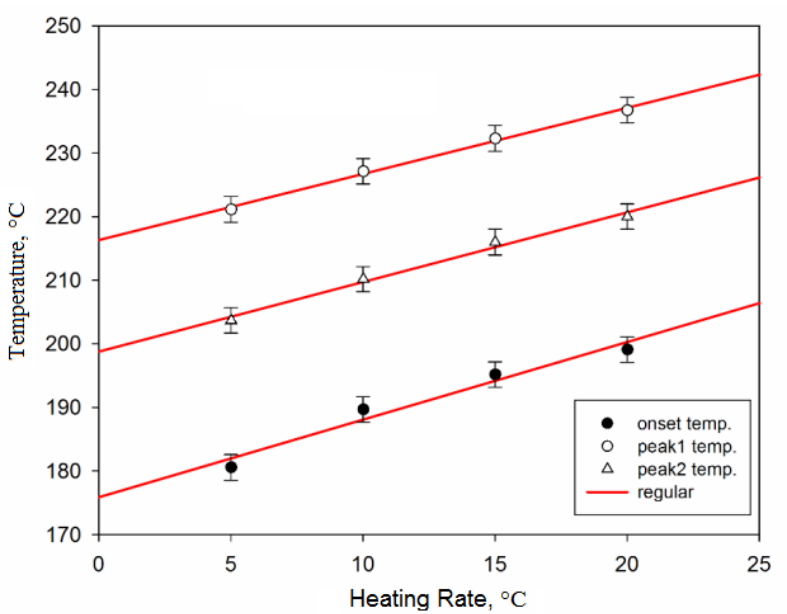

Figure 10. Variation of the peak temperature and onset temperature of GAP-g-PGN with the heating rate

3.3 Thermal decomposition kinetics of GAP-g-PGN

The thermal stability and activation energy of degradation of the polymer was studied by the TG technique. The programmed TG curves under argon for the plasticizer and modified GAP, GAP-g-PGN, are shown in Figure 5. The plasticizer and modified GAP are stable up to approximately 170 °C. These results show that the plasticizer and modified GAP have approximately the same onset degradation temperature. The modified GAP decomposes in two stages around 207 and 300 °C. The initial mass loss of about 43% corresponds to the release decomposition of $–ONO_2$ and $–N_3$ groups, which are exothermic decompositions as understood from the DSC thermograms. The second mass loss corresponds to the slow decomposition of the rest of the polymer. The latter mass loss stage occurs without any considerable heat liberation as there is no exothermic peak observed after the decomposition of the energetic groups.

There are many well-known ways to perform kinetic studies of the degradation of polymeric materials. TG in combination with model-free methods is widely used [28-31]. In the Kissinger method, for example, the temperature at the maximum in the derivative weight loss signal (T_m) of experiments at different heating rates (β) is used. $\ln(\beta/T_m^2)$ is plotted as a function of the reciprocal temperature, and the slope is proportional to the activation energy (E_a) of the degradation step, according to Equation 1 [32, 33].

$$\ln\left(\frac{\beta}{T_m^2}\right) = \ln\frac{AR}{E_a} - \frac{E_a}{RT_m} \tag{1}$$

TGA thermogram illustrates the variation of sample mass with temperature in percent, which is calculated by Equation 2, as a function of the temperature or time. Also, it can be shown as the derivative of mass loss curve *versus* temperature.

$$\text{mass (\%)} = \frac{(m_t - m_e)}{(m_b - m_e)} \tag{2}$$

where m_t is the mass at a specified reaction time, m_b is the mass at the beginning and m_e is the mass at the end of the degradation step or steps.

Figure 8 shows the GAP-g-PGN DSC thermograms obtained at various heating rates. In Figure 11, the corresponding Kissinger plot is depicted with activation energies for degradation of the modified GAP. It was found that the plot of $\ln(\beta/T_m^2)$ against $1000/T_m$ was a straight line, which indicates that the mechanism of thermal decomposition is first order and that

the mechanism of thermal decomposition of GAP-g-PGN does not vary during the decomposition at various heating rates [34]. The slope of the line is equal to $-E_a/R$. Therefore, the activation energy (E_a) was obtained from the slope of the graph [35] (see Figure 11). The results obtained for the activation energy (E_a) and other kinetic parameters for the two steps are listed in Table 3.

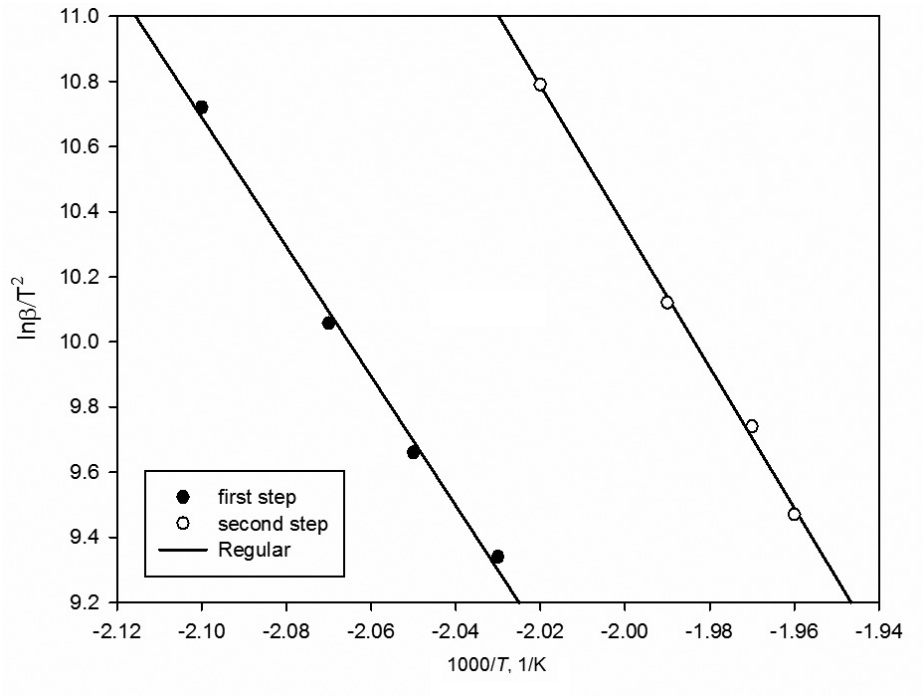

Figure 11. The plot of $\ln\beta/T_m^2$ *versus* $1/T_m$ (Kissinger method)

Table 3. Kinetic parameters of GAP-g-PGN

Step	T_p [°C]	E_a [kJ/mol]	R^2	lnA [s^{-1}]
Peak 1 (ONO_2)	203	165	0.995	40.86
Peak 2 (N_3)	220	179	0.998	43.00

Knowing the value of the frequency factors (A) and E_a for a given temperature, the rate constant (k) for the decomposition reaction of GAP-g-PGN can be calculated by Equation 3.

$$k = Ae^{-E_a/RT} \tag{3}$$

So this parameter is important for the estimation of ageing, thermal stability, and mechanism of *decomposition of* energetic materials [36]. Equation 3 can be solved for a temperature of 50 °C using E_a and A. The results of the kinetic parameters for GAP-g-PGN are summarized in Table 3.

A second model-free approach is the analysis of isothermal and linear non-isothermal TG measurements by an isoconversional method, *i.e.* the Flynn-Wall-Ozawa (FWO) method. For constant heating rates, the activation energy (E_α) is determined from the slope of the logarithm of the heating rate (logβ) *versus* the reciprocal temperature corresponding to a selected conversion degree α ($1/T_\alpha$), according to Equation 4 [37-39].

$$\log \beta = C - \left(0.4567 \frac{E_\alpha}{RT_\alpha}\right) \tag{4}$$

where T_α is the temperature at conversion degree (α), and C is a constant. According to the FWO method (Equation 4), the activation energy (E_α) can be obtained at each degree of degradation (α) from the slope of the logβ *versus* $1/T$ plot (Figure 12).

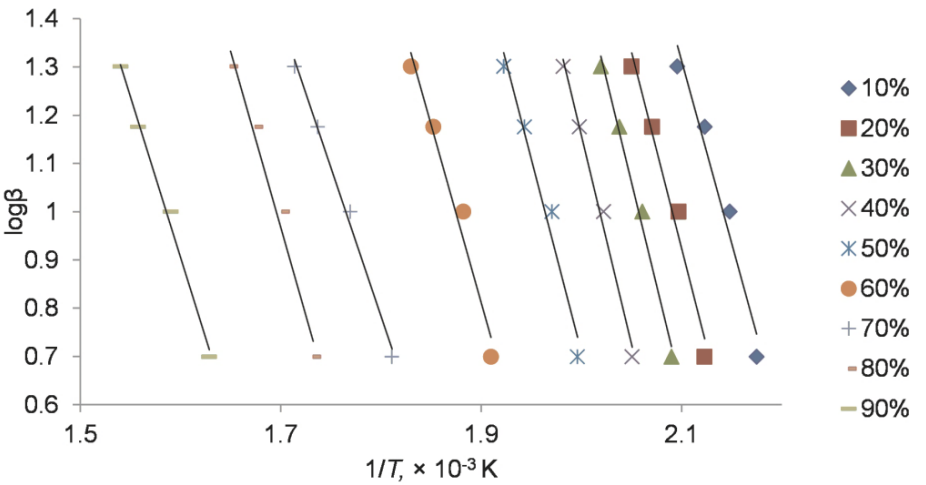

Figure 12. Plots of logβ against $1/T$ (FWO method) for selected values of conversion

Figure 13 shows the dependence of the activation energy on the degree of degradation evaluated for the non-isothermal data (linear heating rate). As the diagram reveals, the activation energy for GAP-g-PGN degradation

increased as the degradation proceeded, reached a maximum value and then decreased.

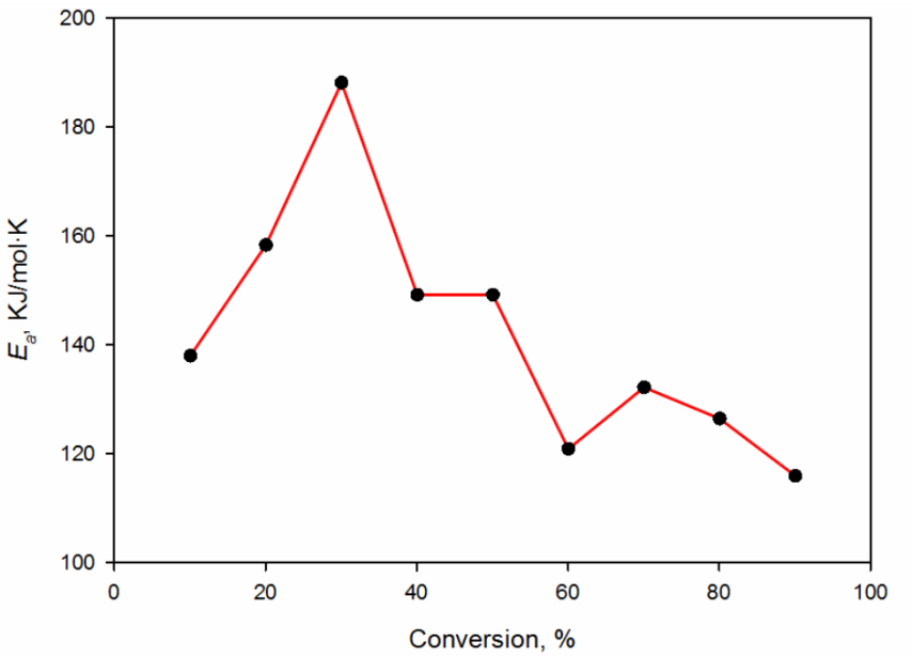

Figure 13. The dependence of E_a on percentage conversion for the thermal decomposition of GAP-g-PGN (FWO method)

The change of activation energy *vs.* conversion percentage has also shown proper fitting of the FWO method. In the first decomposition step, cleavage of the nitrate groups of PGN pendant chain produces an alkoxide radical and NO_2, but at 30% conversion NO_2 plays the role of a catalyst for the decomposition of the nitrate group and reduces the activation energy of decomposition. In the second decomposition step, the azidomethyl groups of GAP-g-PEG decompose to a nitrene *via* loss of N_2, and subsequent insertion of the reactive intermediate into a C–H bond to afford an imine (Figure 14).

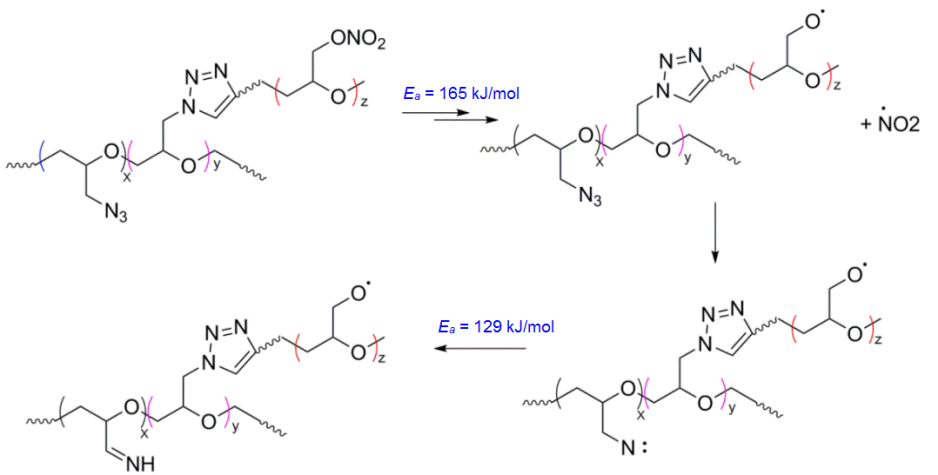

Figure 14. Proposed mechanism for the first and second steps of GAP-g-PGN decomposition

3.4 Thermal decomposition thermodynamics of GAP-g-PGN

The thermodynamic parameters of GAP-g-PGN decomposition were calculated from Equations 6-8, and the results are listed in Table 4.

$$k = \frac{K_B}{h} \exp \frac{-\Delta G‡}{RT} \quad (6)$$

$$\Delta H‡ = E_a - RT \quad (7)$$

$$\Delta G‡ = \Delta H‡ - T\Delta S‡ \quad (8)$$

where k is the reaction rate constant in s^{-1}, $\Delta G‡$ is the free energy in kJ/mol, $\Delta H‡$ is the enthalpy in kJ/mol, $\Delta S‡$ is the entropy in J/mol·K, h is Planck's constant, and K_B is Boltzmann's constant [40].

Table 4. Thermodynamic parameters of GAP-g-PGN

T	$\Delta G‡$ [kJ/mol]	$\Delta H‡$ [kJ/mol]	$\Delta S‡$ [J/(mol·K)]
T_{p1}	159	161	4.22
T_{p2}	178	175	6.08

3.5 Critical explosion temperature

For safe storage and process operations, one of the important parameters for energetic materials such as propellants is the critical explosion temperature (T_b). This is defined as the lowest temperature to which a specific charge may be heated without undergoing thermal runaway [41, 42]. T_b may be calculated

from inflammation theory and appropriate thermokinetic parameters, namely the activation energy, the pre-exponential factor, and the heat of reaction. To obtain T_b for GAP-g-PGN, Equations 9 and 10 were used [43].

$$T_e = T_{e0} + a\beta_i + b\beta_i^2 \text{ , where } i = 1\text{-}4 \tag{9}$$

$$T_b = \frac{E_a - \sqrt{E_a^2 - 4E_a R T_{e0}}}{2R} \tag{10}$$

where a and b are coefficients, β_I is the heating rate, R is the universal gas constant (8.314 J/K·mol), and E_a is the activation energy. T_{e0} is defined as the onset temperature (T_e) corresponding to $\beta_I \rightarrow 0$ by Equation 9. The plot of the onset temperature *versus* the heating rate was fitted as second-order with $R^2 = 0.995$ (Figure 9). Then T_{e0} was obtained as 188.56 ±0.05 °C for the 20% modified GAP. Values of T_b obtained from Equation 10 were 182.02 ±0.05 and 182.23 ±0.05 °C for the 20% modified GAP by using FWO and Kissinger data, respectively.

The self-accelerating decomposition temperature (T_{SADT}) is an important parameter that characterizes the thermal hazard under transport conditions of condensed self-reactive substances. The T_{SADT} value is a very important parameter for assessing the safe management of reactive substances in storage, transportation, and use. It is defined as the lowest temperature at which self-accelerating decomposition may occur in a reactive substance packed for transportation purposes. The T_{SADT} value determines whether the substance should be subject to temperature control during transport. The T_{SADT} value was estimated using the kinetic parameters, based on the Semenov model. Equation 11 was used [44, 45] to obtain the self-accelerating decomposition temperature (T_{SADT}) for GAP-g-PGN.

$$T_{SADT} = T_b - \frac{RT_b^2}{E_a} \tag{11}$$

where T_e is the thermal explosion temperature, R is the universal gas constant, E_a is the activation energy (J/mol). The T_{SADT} value obtained from Equation 11 was 173 and 172 ℃ for the 20% modified GAP using FWO and Kissinger data, respectively.

4 Conclusions

A reactive energetic plasticizer was synthesized in good yield. This plasticizer was reacted *via* Cu- free conditions, by a click reaction with GAP and afforded GAP-g-PGN as a likely energetic binder.

The TGA/DTG results showed that the thermal degradation of this energetic copolymer occurs in three steps, related to the thermal degradation of the nitrate ester groups, the azidomethyl groups, and the polyether skeleton, respectively. The peaks for each stage were at 200, 220 and 285 °C. In addition, the thermal decomposition kinetics were determined by the Kissinger method and have shown the activation energies for these three decomposition steps are 165.12 ±0.05, 179.74 ±0.05 and 147.99 ±0.05 kJ/mol, respectively.

The glass transition temperature (T_g) value of GAP-g-PGN was lower than the initial GAP. The critical temperature of thermal explosion (T_b) was 182.02 ±0.05 and 182.23 ±0.05 °C using FWO and Kissinger data, respectively. The self-accelerating decomposition temperature (T_{SADT}) was 172.86 ±0.05 and 171.97 ±0.05 °C using FWO and Kissinger data, respectively.

References

[1] Kohga, M. From Cross-linking to Plasticization – Characterization of Glycerin/HTPB Blends. *Propellants Explos. Pyrotech*. **2009**, *34*(5): 436-443.

[2] Shankwalkar, S.G.; Cruz, C. Thermal Degradation and Weight Loss Characteristics of Commercial Phosphate Esters. *Ind. Eng. Chem. Res*. **1994**, *33*(3): 740-743.

[3] Gowariker, V.R.; Viswanathan, N.V.; Sreedhar, J. *Polymer Science*. 2nd ed., New Age International **2015**; ISBN 0470203226.

[4] Frankel, E.N.; Pryde, E.H. *Acetoxymethyl Derivatives of Polyunsaturated Fatty Triglycerides as Primary Plasticizers for Polyvinylchloride*. Patent US 4083816A, **1978**.

[5] Wypych, G. *Handbook of plasticizers*. 3rd ed., ChemTec Publishing, Elsevier **2017**: P.27; ISBN 9781895198973.

[6] Bohn, M.A. Determination of the Kinetic Data of the Thermal Decomposition of Energetic Plasticizers and Binders by Adiabatic Self-heating. *Thermochim. Acta* **1999**, *337*(1-2): 121-139.

[7] Kumari, D.; Balakshe, R.; Banerjee, S.; Singh, H. Energetic Plasticizers for Gun and Rocket Propellants. *Rev. J. Chem.* **2012**, *2*(3): 240-262.

[8] Chen, Y.; Kwon, Y.; Kim, J.S. Synthesis and Characterization of *bis*(2,2-Diisopropylethylene) Formal Plasticizer for Energetic Binders. *J. Ind. Eng. Chem*. **2012**, *18*(3): 1069-1075.

[9] Provatas, A. Energetic Plasticizer Migration Studies. *Energ. Mater.* **2003**, *21*(4): 237-245.
[10] Marcilla, A.; García, S.; Garcia-Quesada, J. Migratability of PVC Plasticizers. *Polym. Test* **2008**, *27*(2): 221-233.
[11] Hakkarainen, M. Migration of Monomeric and Polymeric PVC Plasticizers. *Adv. Polym. Sci*. **2008**, *211*: 159-185.
[12] Zhou, Y.; Long, X.; Wei, X. Theoretical Study on the Diffusive Transport of 2,4,6-Trinitrotoluene in the Polymer-bonded Explosive. *J. Mol. Model*. **2011**, *17*: 3015-3019.
[13] Nair, U.; Asthana, S.; Rao, A.S.; Gandhe, B. Advances in High Energy Materials. *Defence Sci. J.* **2010**, *60*(2): 137-151.
[14] Yang, B.; Bai, Y.; Cao, Y. Effects of Inorganic Nano-particles on Plasticizers Migration of Flexible PVC. *J. Appl. Polym. Sci*. **2010**, *115*(4): 2178-2182.
[15] Bodaghi, A.; Shahidzadeh, M. Synthesis and Characterization of New PGN Based Reactive Oligomeric Plasticizers for Glycidyl Azide Polymer. *Propellants Explos. Pyrotech.* **2018**, *43*: 364-370.
[16] Mohan, Y.M.; Raju, M.P.; Raju, K.M. Synthesis, Spectral and DSC Analysis of Glycidylazide Polymers Containing Different Initiating Diol Units. *J. Appl. Polym. Sci*. **2004**, *93*(5): 2157-2163.
[17] Liu, D.; Zheng, Y.; Steffen, W.; Wagner, M.; Butt, H.J.; Ikeda, T. Glycidyl 4-Functionalized-1,2,3-triazole Polymers. *Macromol. Chem. Phys.* **2013**, *214*(1): 56-61.
[18] Song, S.; Ko, Y.-G.; Lee, H.; Wi, D.; Ree, B.J.; Li, Y.; Michinobu, T.; Ree, M. High-Performance Triazole-containing Brush Polymers *via* Azide-Alkyne Click Chemistry: A New Functional Polymer Platform for Electrical Memory Devices. *NPG Asia Mater.* **2015**, *7*(e288): 228-240.
[19] Shee, S.K.; Reddy, S.T.; Athar, J.; Sikder, A.K.; Talawar, M.; Banerjeeb, S.; Khan, S. Probing Plasticizers: Thermal, Rheological, and DFT Studies, the Compatibility of Energetic Binder Poly Glycidyl Nitrate with Energetic Plasticizer. *RSC Adv*. **2015**, *5*(123): 101297-101308.
[20] Pant, C.S.; Wagh, R.M.; Nair, J.K.; Gore, G.M.; Venugopalan, S. Synthesis, and Characterization of Two Potential Energetic Azido Esters. *Propellants Explos. Pyrotech*. **2006**, *31*(6): 477-481.
[21] Kumari, D.; Anjitha, S.; Pant, C.S.; Patil, M.; Singh, H.; Banerjee, S. Synthetic Approach to Novel Azido Esters and Their Utility as Energetic Plasticizers. *RSC Adv.* **2014**, *4*(75): 39924-39933.
[22] Ang, H.G., Pisharath, S. *Energetic Polymers.* Wiley-VCH, Weinheim/Chichester, **2012**; ISBN 9783527331550.
[23] Shaojun, Q.; Huiqing, F.; Chao, G.; Xiaodong, Z.; Xiaoxian, G. An Azido Ester Plasticizer 1,3-Di(Azidoacetoxy)-2,2-Di(Azidomethyl) Propane (PEAA): Synthesis, Characterization and Thermal Properties. *Propellants Explos. Pyrotech*. **2006**, *31*(3): 205-208.
[24] Drees, D.; Löffel, D.; Messmer, A.; Schmid, K. Synthesis and Characterization of Azido Plasticizer. *Propellants Explos. Pyrotech*. **1999**, *24*(3): 159-162.

[25] Zhang, Z.; Wang, G.; Luo, N.; Huang, M.; Jin, M.; Luo, Y. Thermal Decomposition of Energetic Thermoplastic Elastomers of Poly(glycidyl nitrate). *J. Appl. Polym. Sci*. **2014**, *131*(21): 40961-40966.
[26] Hai, C. The Investigation of Thermal Decomposition Kinetics for PNIMMO by TG-MS. *Initiators and Pyrotechnics*. **2007**, *2*(4): 32-35.
[27] Mohan, Y.M.; Raju, K.M.; Sreedhar, B. Synthesis and Characterization of Glycidylazide Polymer with Enhanced Azide Content. *Int. J. Polym. Mater*. **2006**, *55*(6): 441-455.
[28] Lua, A.C.; Su, J. Isothermal and Non-isothermal Pyrolysis Kinetics of Kapton® Polyimide. *Polym. Degrad. Stab*. **2006**, *91*(1): 144-153.
[29] Sivalingam, G.; De, P.; Karthik, R.; Madras, G. Thermal Degradation Kinetics of Vinyl Polyperoxide Copolymers. *Polym. Degrad. Stab*. **2004**, *84*(1): 173-179.
[30] Morancho, J.; Salla, J.; Ramis, X.; Cadenato, A. Comparative Study of the Degradation Kinetics of Three Powder Thermoset Coatings. *Thermochim. Acta* **2004**, *419*(1): 181-187.
[31] Flynn, J.H.; Wall, L.A. A Quick Direct Method for the Determination of Activation Energy from Thermogravimetric Data. *J. Polym. Sci. Pol. Lett*. **1966**, *4*(5): 323-328.
[32] Kissinger, H.E. Reaction Kinetics in Differential Thermal Analysis. *Anal. Chem*. **1957**, *29*(11): 1702-1706.
[33] Chizari, M.; Bayat, Y. Synthesis and Kinetic Study of a PCL-GAP-PCL Tri-block Copolymer. *Cent. Eur. J. Energ. Mater.* **2018**, *15*(2): 243-257.
[34] Salla, J.; Morancho, J.; Cadenato, A.; Ramis, X. Non-isothermal Degradation of a Thermoset Powder Coating in Inert and Oxidant Atmospheres. *J. Therm. Anal. Calorim*. **2003**, *72*(2): 719-728.
[35] Li, L.; Guan, C.; Zhang, A.; Chen, D.; Qing, Z. Thermal Stabilities and the Thermal Degradation Kinetics of Polyimides. *Polym. Degrad. Stab.* **2004**, *84*(3): 369-373.
[36] Shekhar, P.C.; Santosh, M.S.; Banerjee, S.; Khanna, P.K. Single-Step Synthesis of Nitro-Functionalized Hydroxyl-Terminated Polybutadiene. *Propellants Explos. Pyrotech*. **2013**, *38*(6): 748-753.
[37] Rantuch, P.; Kačíková, D.; Nagypál, B. Investigation of Activation Energy of Polypropylene Composite Thermooxidation by Model-free Methods. *Eur. J. Environ. Saf. Sci.* **2014**, *2*(1): 12-18.
[38] Wang, H.; Tao, X.; Newton, E. Thermal Degradation Kinetics and Lifetime Prediction of a Luminescent Conducting Polymer. *Polym. Int.* **2004**, *53*(1): 20-26.
[39] Wan, C.; Tian, G.; Cui, N.; Zhang, Y.; Zhang, Y. Processing Thermal Stability and Degradation Kinetics of Poly(vinyl Chloride)/Montmorillonite Composites. *J. Appl. Polym. Sci*. **2004**, *92*(3): 1521-1526.
[40] Olszak-Humienik, M.; Mozejko, J. Thermodynamic Functions of Activated Complexes Created in Thermal Decomposition Processes of Sulphates. *Thermochim. Acta* **2000**, *344*(1-2): 73-79.
[41] Pickard, J.M. Critical Ignition Temperature. *Thermochim. Acta* **2002**, *392-393*: 37-40.
[42] Rodgers, R.N.; Janney, J.L.; Ebinger, M.H. Kinetic-isotope Effects in Thermal Explosions. *Thermochim. Acta* **1982**, *59*(3): 287-298.

[43] Zhang, T.L.; Hu, R.Z.; Xie, Y.; Li, F.P. The Estimation of Critical Temperatures of Thermal Explosion for Energetic Materials using Non-isothermal DSC. *Thermochim. Acta* **1994**, *244*: 171-176.
[44] Dong, J.; Ou, J.-Y.; Zhu, L.; Li, B. Thermal Decomposition Kinetic Study of Azido-terminated Glycidyl Azide Polymer. *Chin. J. Energ. Mater.* (*Hanneng Cailiao)* **2016**, *24*(6): 555-559.
[45] Sun, J.; Li, Y.; Hasegawa, K. A Study of Self-accelerating Decomposition Temperature (SADT) using Reaction Calorimetry. *J. Loss Prevent. Proc.* **2001**, *14*(5): 331-336.

Received: June 27, 2018
Revised: June 13, 2019
First published online: June 27, 2019